COMPARATIVE ANALYSIS OF COOLING EFFECT OF BATTERY MODULE COOLING PLATE STRUCTURES

by

Haifeng FANG[a,b*], Juncheng XU[a], Yiqiang LU[c], Mingqiang WANG[a], and Xin LI[c]

[a]College of Mechanical Engineering, Jiangsu University of Science and Technology, Zhenjiang, Jiangsu, China
[b]Suzhou Institute of Technology, Jiangsu University of Science and Technology, Zhangjiagang, Jiangsu, China
[c]Jiangsu Keyi New Energy Technology CO., LTD,Zhangjiagang, Jiangsu, China

Original scientific paper
https://doi.org/10.2298/TSCI230520166F

In order to investigate the impact of cooling plate channel structural parameters on the cooling performance of battery modules, a heat generation model for $LiFePO_4$ batteries was established. Based on the model, the 1C discharge process of $LiFePO_4$ batteries at room temperature (25 °C) was simulated, and relevant heat release data were obtained. On this basis, three different cooling plate structures (Model A, Model B, Model C) were designed, and the cooling performance of the cooling liquid (50% water and 50% ethylene glycol) for the battery module was analyzed by simulation at different mass-flow rates (0.15 kg/s, 0.18 kg/s, 0.21 kg/s), along with the pressure, temperature difference and flow rate of the cooling channel. The results showed that the uniformity of the flow rate in the channel can reduce the temperature difference. Under the same mass-flow rate, the temperature difference of the battery module on the same surface between Model A and Model C was 1.1 °C, but too many channels would increase the pressure drop. The pressure drop of Model C was more than 10 times that of Model B. Therefore, it is necessary to design the channel structure reasonably while ensuring the heat dissipation effect. Finally, based on the simulation results, beneficial suggestions for the cooling and cooling plate design and manufacture of energy storage container battery modules are proposed.

Key words*: $LiFePO_4$ battery module, heat dissipation structure, pressure, battery heat release*

Introduction

Because of its long lifespan, high temperature tolerance, large capacity, and pollution-free characteristics, $LiFePO_4$ battery [1] are widely used in energy storage systems. Additionally, they do not explode even in the case of severe collisions. Due to its low cost and high rate capabilities, $LiFePO_4$ battery also have great potential in power-type applications.

The cell is the basic unit of a battery module and produces a lot of heat during the chemical reaction. Therefore, the lifespan, energy output, and temperature of the battery are strongly related. A good battery thermal management system can improve battery performance, so the design of the thermal management system is crucial.

*Corresponding author, e-mail: fanghale@163.com

Battery thermal management technology [2] can usually be divided into air cooling [3], liquid cooling [4], PCM cooling [5], heat pipe cooling [6], and mixed cooling. However, air cooling is unable to achieve uniform heat dissipation for large-capacity battery modules and can only be used in simpler structures. The PCM cooling requires the use of other cooling methods, while heat pipe cooling has complex systems and leakage risks and is still in the laboratory design stage. Compared with other cooling methods, liquid cooling has the advantages of low cost and simple structure and is widely used in large battery module heat dissipation.

The $LiFePO_4$ battery have widespread applications and are currently used in passenger cars, energy storage containers [7], with liquid cooling typically used for battery module cooling. There are many factors to consider for liquid cooling battery module, such as the manufacturing process of the cooling plate [8], the pressure it can withstand and its flow resistance, as they all affect the cooling effect of the battery module.

Optimization of battery module heat dissipation has always been a concern for researchers, and optimization design of the battery module cooling has been extensively covered in literature. For example, Ravindra *et al.* [9] designed a new cooling plate and used mixed cooling to reduce the battery temperature difference and the average temperature difference between adjacent batteries. Wang *et al.* [10] compared the series and parallel cooling methods of battery module to balance the temperature of the battery module. Guo *et al.* [11] optimized the flow path's structure and flow rate through orthogonal experimental data and demonstrated that flow rate and flow path width significantly affect battery heat dissipation. Zhang *et al.* [12] increased the fins on the liquid cooling channel and optimized the layout and height of the fins to demonstrate that adding fins can improve battery thermal management performance. Fang *et al.* [13] designed heat pipe structures around soft pack lithium batteries to achieve local heat dissipation effects. Ding, *et al.* [14] demonstrated that optimizing mass-flow rate, temperature, and cooling plate width can improve cooling performance while reducing pump energy consumption. Behi *et al.* [15] installed heat pipes to demonstrate that mixed cooling can improve battery module cooling capacity. Asif *et al.* [16] reduced battery module temperature by optimizing heat generation, conductivity ratio, Reynolds number, spacing between the packs, and coolant Prandtl number.

To explore the effect of cooling plate structure on the cooling performance of $LiFePO_4$ battery modules in depth and verify the improvement of cooling performance of battery modules by changing the structure of cooling plate, multiple cooling plate models were established and simulated with corresponding mass-flow rates for the battery module. The effects of changes in cooling plate structure and cooling liquid mass-flow rate on the cooling performance of the battery module were analyzed separately while keeping the battery module unchanged. From the experimental results, it is determined that the fin-type runner is chosen as the final cooling plate model. It is also concluded from the experimental results and the reference paper of Feng *et al.* [17] that by optimizing the number of fins and the thickness of fins will make the heat dissipation performance more better, so the temperature of the battery module will be further reduced by optimizing the structural parameters later.

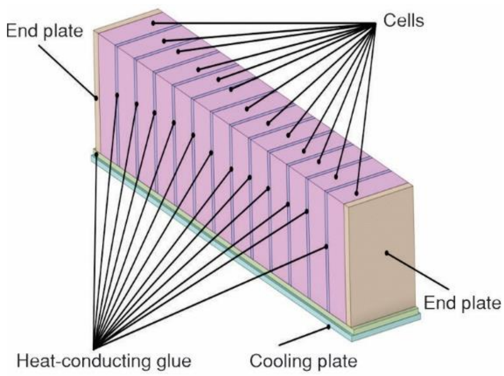

Figure 1. Overall layout of battery

Model establishment

Introduction to the model

The battery pack model is shown in fig. 1, and the cooling plate is made of 2 mm thick aluminum plate, which is widely used for battery module cooling due to its good thermal conductivity, ease of processing, and low cost. The battery module consists of 13 $LiFePO_4$ batteries . Heat conducting glue (Hui Tian 8658) is coated between the batteries , between the batteries and the cooling plate for heat transfer. The main material parameters are shown in tab. 1.

Table 1. Parameters of the material used in battery module structure

Material	Density [kgm^{-3}]	Thermal conductivity [Wm^{-1}K^{-1}]	Specific heat [Jkg^{-1}K^{-1}]
Aluminum	2702	236	903
Heat conducting glue	1550	1.8	1.457
Cooling liquid	1069.4	0.4	3358

This article selects a 280 Ah $LiFePO_4$ battery module as the research object, and the main parameters of the battery are detailed in tab. 2. Considering the flow channel structure of the cooling plate and the mass-flow rate of the cooling fluid, three different cooling plate structures were designed, namely the linear type (Model A), fin type (Model B), and serpentine type (Model C). These three models [17] are widely used in the cooling system of battery modules and have the advantage of simple manufacture and low processing cost, with good cooling effects in energy storage systems and automotive cooling. The specific parameters of the cooling plate can be found in fig. 2.

Table 2. Parameters of 280Ah LiFePO4 Battery

Parameters	Values
Rated capacity [Ah]	280
Rated voltage [V]	3.2
Internal resistance [mΩ]	≤1.0
Specific heat capacity [Jkg^{-1}K^{-1}]	1029.49
Size of cell (length × width × height) [mm]	174 × 71 × 207
Thermal conductivity (*X*-, *Y*-, *Z*-directions) [Wm^{-1}K^{-1}]	21.63/2.11/21.63

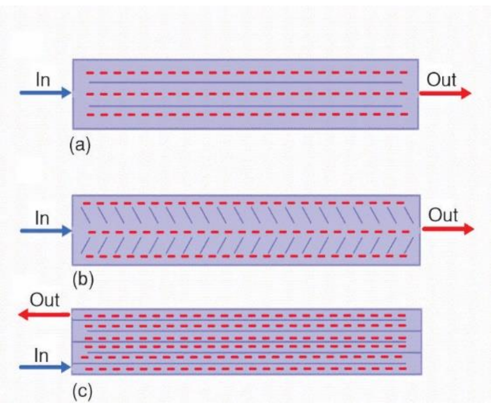

Figure 2. Cooling plate flow channel structure diagram; (a) Model A, (b) Model B, and (c) Model C

Equation

During charging of a $LiFePO_4$ battery, lithium ions Li+ in the positive electrode migrate towards the negative electrode through a polymer separator; during discharging, lithium ions Li+ in the negative electrode migrate towards the positive electrode through the separator. The chemical reaction equation for a $LiFePO_4$ battery [11] can be given:

– Positive electrode

$$\mathrm{LiFePO_4} \underset{\text{Discharge}}{\overset{\text{Charge}}{\rightleftharpoons}} x\mathrm{Li}^+ + \mathrm{Li}_{(1-x)}\mathrm{FePO_4}$$

– Negative electrode

$$6\mathrm{C} + x\mathrm{Li}^+ + xe^- \underset{\text{Discharge}}{\overset{\text{Charge}}{\rightleftharpoons}} \mathrm{Li}_x\mathrm{C}_6$$

– Total reaction

$$\mathrm{LiFePO_4 + 6C \underset{Discharge}{\overset{Charge}{\rightleftarrows}} Li_{(1-x)}FePO_4 + Li_xC_6}$$

When modeling the thermal characteristics of a battery, it is often assumed that the battery is an anisotropic homogeneous solid, and that heat is generated uniformly and is not affected by the direction of the current. According to the Bernardi [18] heat model, lithium-ion batteries generate energy through chemical reactions, with the main reaction producing heat. In addition to this primary heat source is Q_r, there are other sources of heat, such as heat generated by non-primary reactions is Q_a, heat generated by the poles is Q_p, and heat generated by internal resistance is Q_J. Assuming that the total amount of heat generated is Q_t, we have:

$$Q_t = Q_r + Q_a + Q_p + Q_J \tag{1}$$

During the charge and discharge process of lithium-ion batteries, the main reaction related to lithium ions produces the main reaction. Lithium-ion batteries need to obtain energy during the charging process, so they are considered negative. The formula for calculating this heat is:

$$Q_r = \frac{nmQI}{MF} \tag{2}$$

where Q_r is the sum of the heat of the main chemical reaction, I [A] – the current, M [gmol^{-1}] – the molar mass, and F – the Faraday's constant (= 9684.5 C/mol).

The heat of $LiFePO_4$ battery mainly comes from two aspects: on the one hand, the heat generated by the slight decomposition of positive and negative electrode materials caused by the flow of electrons during battery discharge, on the other hand, the heat generated by the thermal decomposition of the electrolyte. Although the exothermic reaction of the battery will cause the temperature to rise and release a certain amount of heat, this part of the heat is not taken into account when considering the main research content.

No matter what the material is, there is a greater or lesser resistance value, and the internal electrolyte also has a certain small resistance value, the formula is:

$$Q_J = I^2 r \tag{3}$$

where r [Ω] is the resistance and I [A] – the current.

When the internal current flows in the battery, the resistance of the electrolyte will cause a pressure difference between the two pole materials, which will generate polarization heat. This heat is irreversible and will not be absorbed or dissipated by the external environment. A formula can be written out in a simple way:

$$Q_t = Q_r + I^2 R + Q_a \tag{4}$$

where $R = r + r_p$, r is the Ohmic resistance. This can be further simplified to:

$$Q_t = Q_r + I^2 r + Q_a \tag{5}$$

The fluid state is determined by the Reynolds number, ρ is the fluid density, V – the fluid velocity, L – the characteristic length (such as the diameter of a circular pipe, length of a flat plate, *etc.*), and μ – the dynamic viscosity of the fluid, which is calculated:

$$\mathrm{Re} = \frac{\rho VL}{\mu} \tag{6}$$

The mass-flow rate is the mass passing through a particular cross-section of the fluid per unit time, usually measured in kg/s, which is calculated:

$$m = \rho VA \tag{7}$$

We can substitute the mass-flow rate formula into the Reynolds number formula and obtain the formula:

$$\mathrm{Re} = \frac{mL}{A\mu} \tag{8}$$

Model validation

The following assumptions are made for the model:
- The battery module is simplified in structure, ignoring the battery pack shell and pole ears, *etc*.
- The battery material is assumed to be evenly distributed, and parameters such as density and specific heat capacity do not vary with time and are taken as the same value.
- The thermal conductivity of the battery is assumed to be anisotropic, with a value equal to the average thermal conductivity in all directions.

In this article, the battery model was simulated by conducting a 1C discharge test at room temperature (25 °C) for a 280 Ah $LiFePO_4$ battery. As shown in fig. 4, according to the experimental results, the temperature difference between the experiment and simulation is a maximum of 1.5 °C, see fig. 3, which indicates that the error of the model is within an acceptable range. The experimental results show that the heat source calculation method is accurate and the CFD numerical model is reliable.

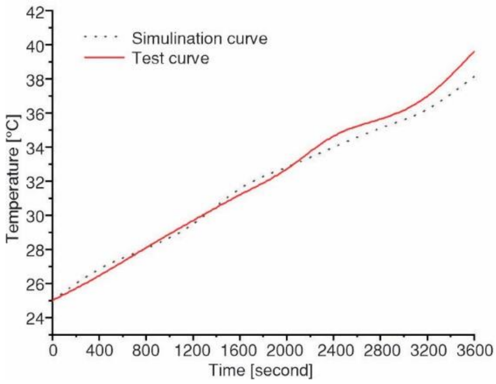

Figure 3. Comparison of battery test and simulation results

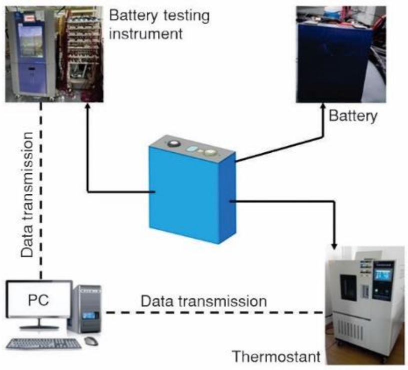

Figure 4. Testing equipment of battery

Boundary condition design

This article simulates the heat dissipation of battery modules under real operating conditions by setting boundary conditions. Different cooling liquid mass-flow rates (0.15 kg/s, 0.18 kg/s, and 0.21 kg/s) with the same cooling liquid temperature were used for simulations under different structures. The inlet of the cooling fluid was set as the flow inlet, and the outlet was set as the pressure outlet. Model A-0.18 means simulating Model A with a mass-flow rate of 0.18 kg/s. The inlet of the coolant is set as a flow inlet, while the outlet is set as a pressure outlet. The temperature of the coolant is set to 18 °C and the ambient temperature is 25 °C. Obtain the heat dissipation results of battery modules with different structures under the same mass-flow rate and at different mass-flow rates under the same structure through experiments.

The accuracy of simulation results is crucial and grid analysis plays an essential role in determining the accuracy and computational speed. Therefore, verifying the grid independence of the model is an indispensable step in the simulation. The article divided the entire module into different grid sizes, increased the number of grids in contact with the battery surfaces to obtain more accurate simulation data. To balance computation time and cost, the article used 2351362, 2349819, and 2368125 grid numbers for the simulation. The grid division of Model A is shown in fig. 5.

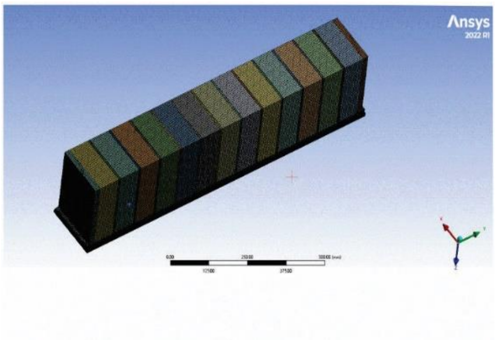

Figure 5. Grid division of Model A

Comparative analysis and discussion of results

By comparing the temperature rise curves of Model A, Model B, and Model C under the same mass-flow rate and temperature conditions, see fig. 7, it can be observed that the temperature rise curve and the final temperature of the battery module do not differ significantly with only a structural change and no other conditions altered. This indicates that the overall temperature difference of the battery modules does not vary greatly due to the overall shape of the cooling plate. Thanks to the impact of the battery material parameters from the manufacturing companies is also a crucial factor, and the effects produced by the same type of battery made by different manufacturers are also different [19].

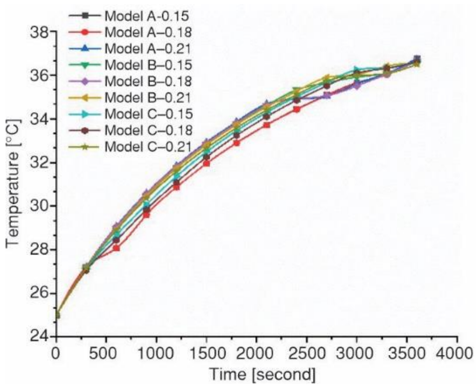

Figure 7. Temperature comparison simulation of different structures at the same mass-flow rate

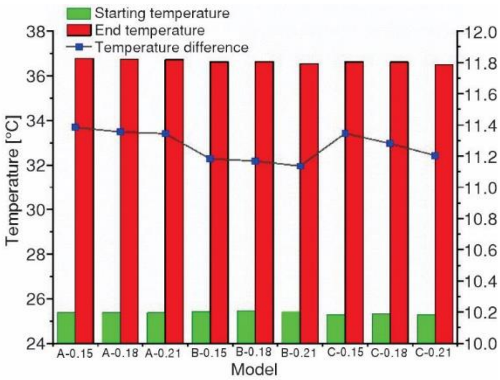

Figure 8. Comparison of temperature difference among battery modules

By examining the effect images of figs. 6 and 8, by observing the cooling effect of the coolant on the battery module and the effect on the temperature, flow rate and pressure of the coolant at the same mass-flow rate. By comparison, when using the same mass-flow rate of 0.18 kg/s in Model A, Model B, and Model C, the temperature difference between them is only 0.186 ℃ (between Model A and Model B) and 0.075 ℃ (between Model A and Model C). As the mass-flow rate increases, the temperature difference among different models gradually becomes larger. However, even when the mass-flow rate is 0.21 kg/s, the maximum temperature difference between Model A and Model B is only 0.208 ℃.

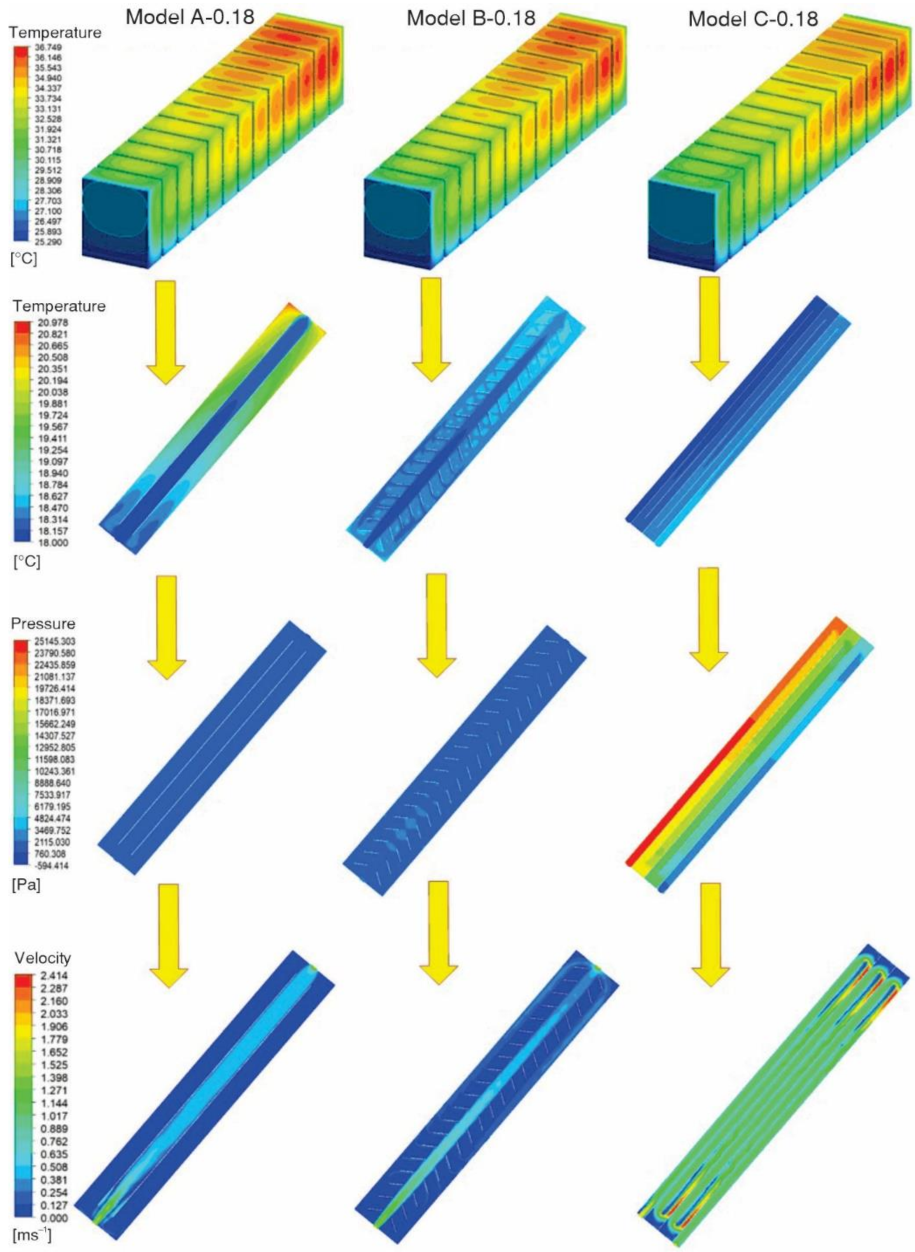

Figure 6. Simulation comparison of different models for temperature, pressure and velocity at a mass-flow rate of 0.18 kg/s

In addition, through the experiment of cooling at different mass-flow rates under the same temperature, it can be seen that as the mass-flow rate increases and the temperature of the battery module is correspondingly improved. Among Model A, Model B, and Model C, the maximum temperature difference occurred when Model C increased from the mass-flow rates of 0.15 kg/s to 0.21 kg/s, which is 0.142 ℃. It can be seen that changes in structure have a greater impact on temperature difference than changes in mass-flow rate alone.

The results in fig. 6 show whether the flow channel structure design is reasonable and whether the cooling liquid can pass through each flow channel. The quality of the flow channel design has a vital role in the heat dissipation of the battery module. Comparing the flow velocity and cooling liquid temperature of Model A, due to the low flow velocity on both sides, the cooling liquid temperature at the outlet on both sides is too high. This also proves that the flow channel design in Model A is unreasonable, which makes the cooling liquid unable to flow towards the outlet uniformly. For Model B, the flow velocity on both sides is higher than that of Model A, but the flow velocity between fins is too low, which leads to poor performance for local heat dissipation of the battery. For Model C, due to the use of a serpentine flow channel, the flow velocity and flow channel temperature are better than those of Model A and Model B.

By comparing the temperature differences between the top and bottom surfaces of the battery module under three different structures, and using the same temperature and mass-flow rate of coolant, see fig. 10, it can be concluded that the cooling channel has a significant impact on the temperature uniformity between the surfaces of the battery module. In the case of a mass-flow rate of 0.15 kg/s, the temperature difference on the lower surface of Model C is smaller than that of Model A by 1.1 °C, and the same is true for the upper surface. Similarly, for Model B, the temperature difference is smaller than that of Model A at 0.15 kg/s. thanks to the Model A, most of the coolant flows into the middle channel, and the flow rate of the channels on both sides is too low, resulting in poor heat dissipation uniformity of the channels. Similarly, for Model B, most of the coolant flows in the middle fins, and there is very little coolant on either side of the fins. Therefore, the temperature difference of Model B is not much different from that of Model A. For Model C, however, its temperature difference is much larger than that of Models A and B, due to the sufficient contact between the channels and the coolant. However, it can also be seen that increasing the mass-flow rate to enhance the heat dissipation effect does not improve the effect significantly - the structural effect is more apparent. Increasing the mass-flow rate has less impact on the heat dissipation of the battery module than changing its structure.

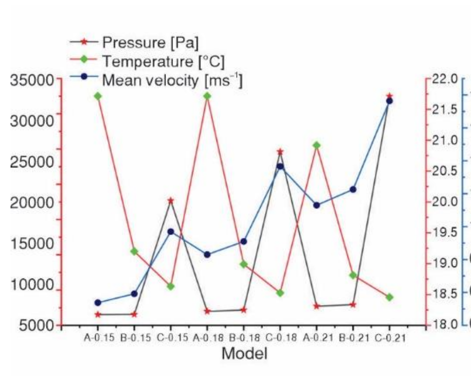

Figure 9. Simulation Comparison of temperature, pressure, and velocity of the channels

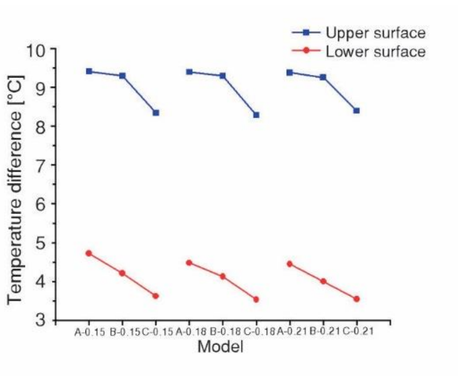

Figure 10. Simulation Comparison of temperature difference between upper and lower surfaces of battery model

While changing the structure of the model did not have a significant impact on the temperature difference of the battery module, the effect of the cooling liquid on the flow channel was significant. It can be seen from figs. 6 and 9 that changing the structure had a great impact on the temperature of the flow channel. Among the three models, in Model A, the maximum temperature difference of the cooling liquid during circulation was 3.715 °C, and the

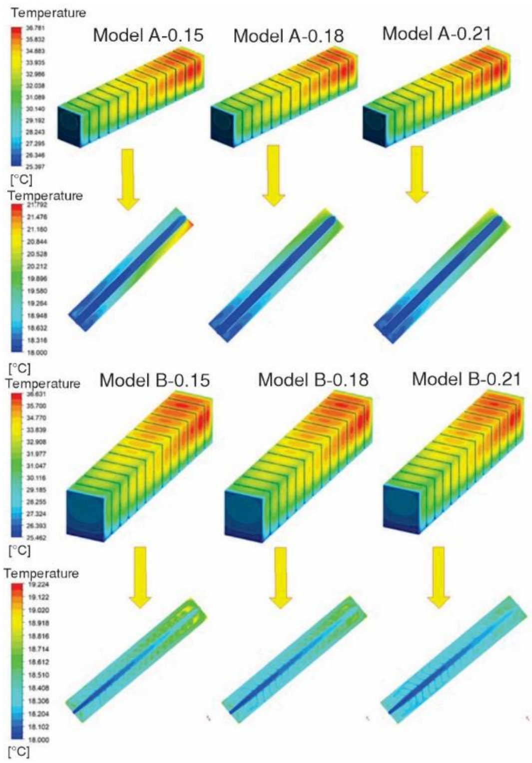

Figure 11. Simulation Comparison of battery module and coolant temperature under different flow rates for Model A and Model B

minimum was 2.917 ℃. However, under the same mass-flow rate, the maximum temperature difference in Model B was only 1.199 ℃, and Model C was even lower at 0.633 ℃. Therefore, increasing the number of flow channels can provide better heat dissipation for the cooling liquid, which helps to reduce the temperature difference of the battery module. As can also be seen from fig. 6, the temperature of the flow channel decreases as the mass-flow rate increases, which can better take away the heat generated by the battery module. Structural changes can better improve the temperature of the battery module than simply increasing mass-flow rate, but changes in structure are not the only factor in performance improvement. As shown in fig. 6, when the mass-flow rate of Model C was increased, the flow resistance increased exponentially, which was due to the increase in the number of flow channels requiring more pressure for the cooling liquid to flow. Model C is several times larger than Model A and Model B at the same mass-flow rate, indicating that under the same conditions, Model C requires a larger power pump to operate. Considering the cooling effect of the model on the battery module and the effect of the cooling liquid on pump power, concluded that the cooling effect of Model C was not significantly better than that of Model A and Model B under the same conditions, and the pressure drop would increase exponentially. Therefore, considering the overall performance, Model C is not suitable for the cooling of battery modules. The following comparison will be conducted between Model A and Model B.

By comparing fig. 11, It can be seen that increasing the mass-flow rate does not have a significant effect on reducing the temperature of the cell module for the same structure, while changing the structure has a greater effect on the temperature than changing the mass-flow rate. From the temperature of the cooling liquid in the flow channel, the temperature of the straight-line Model A flow channel is higher than that of the fin-shaped Model B. Due to the position of the inlet in the middle of the cooling plate, It can be clearly seen that the temperature of the middle runner of Model A and model B is lower than the temperature of both sides. In fig. 12, can be seen as the fins, the temperature of the cooling liquid in Model B is lower than that of Model A. Thus, the temperature of the battery module is lower and the cooling effect is better. It can be seen that by optimizing the angle and length of the fins, the temperature of the battery module can be reduced further and the cooling effect can be improved.

By comparing the influence of the cooling liquid on the flow channel pressure under different mass-flow rates, fig. 13 shows that as the mass-flow rate increases, the maximum pressure of the cooling plate increases, but it is still not as high as that of the flow channel in Model C. Therefore, a pump with small power can be selected to save cost. As can be seen from

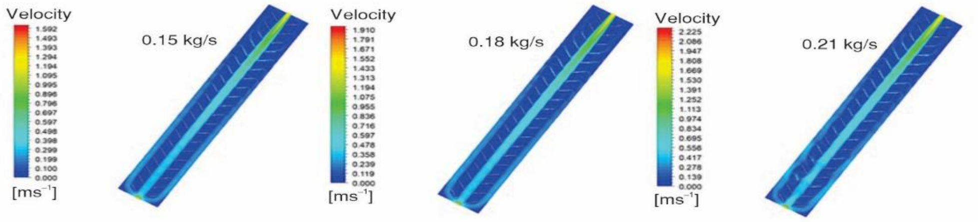

Figure 12. Simulation comparison of channel velocity for Model B at different mass-flow rates

the figure, that the pressure of Model A and Model B at the same mass-flow rate is not significantly different.

Taking into account the performance of the three models in terms of flow rate, pressure, temperature, and cooling performance of the battery module, although Model C has good cooling effect, its flow channel pressure is too high, requiring a larger pump power. The cooling effect of Model A is lower than that of Model B, thus Model B has better overall performance than Model A and Model C. Model B is more effective for cooling the battery module.

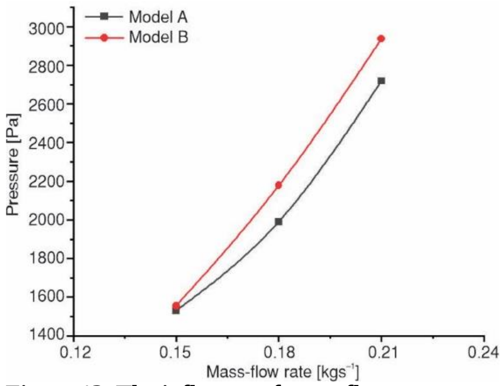

Figure 13. The influence of mass-flow rates on channel pressure

Conclusions

In this study, the phenomenon of temperature rose in $LiFePO_4$ battery during 1C discharge at room temperature was explored by using both simulation and experimental methods. Through thermal analysis of the battery module, the final structure of the cooling plate was determined. The study found that, for the same structure, the cooling plate's structural form was superior to the cooling effect of mass-flow rate on the battery module by compared the cooling effect and flow channel's mass-flow rate, temperature, and pressure at different mass-flow rates. At the same time, a comparison was made using different structures with the same mass-flow rate. Through two different angles of comparison, it was found that the cooling effect of Model B was better than Model A and Model C. The temperature distribution is more uniform, although Model C has a smaller temperature difference during the cooling of the battery module and coolant circulation. However, with too many flow channels, the coolant requires a larger pump power to work, and too many flow channels will also result in higher manufacturing costs for the cooling plate. Therefore, under the condition of satisfying the cooling plate's structural strength, selecting Model B as the final structure of the cooling plate for the battery module has good cooling efficiency and economy. There are many aspects that affect the heat dissipation temperature of the battery module, it is related to the material of the battery, and also related to the winding of the battery, due to the limitation of the cooling plate processing process will also affect its temperature, in future research, the bottom heat dissipation of the battery module can be changed to both sides of the heat dissipation, due to the contact area will have a better heat dissipation effect. In the next study, the structure of model B will be further improved to increase the mass-flow rate between the fins and on both sides by optimizing the number, length and angle of the fins, which will result in better thermal performance of the battery module.

Acknowledgment

This work is financially supported by Qing Lan project of the Higher Education Institutions of Jiangsu Province and Science, Technology Plan Project of Jiangsu Province (International Science and Technology Cooperation Special Fund) (BZ2022029) and Jiangsu Keyi New Energy Technology CO., LTD.

References

[1] Song, L., *et al*., Thermal Runaway Propagation Behavior and Energy Flow Distribution Analysis of 280 Ah $LiFePO_4$ Battery, *Process Safety and Environmental Protection, 170* (2023), Feb., pp. 1066-1078
[2] Hajialibabaei, M., *et al*., A Critical Review of the Straight and Wavy Microchannel Heat Sink and the Application in Lithium-Ion Battery Thermal Management, *Int. J. of Thermofluids, 14* (2022), 100153
[3] Lv, Y., *et al*., A Novel Thermal Management Structure Using Serpentine Phase Change Material Coupled with Forced Air Convection for Cylindrical Battery Modules, *J. of Power Sources, 468* (2020), 228398
[4] Mokashi, I., *et al*., Maximum Temperature Analysis in a Li-Ion Battery Pack Cooled by Different Fluids, *Journal of Thermal Analysis and Calorimetry, 141* (2020), 6, pp. 2555-2571
[5] Ravindra, J., *et al*., A Novel Battery Thermal Management System Using Nano-Enhanced Phase Change Materials, *Energy, 219* (2021), 119564
[6] Jiaqiang, E., *et al*., Effect Analysis on Heat Dissipation Performance Enhancement of a Lithium-Ion-Battery Pack with Heat Pipe for Central and Southern Regions in China, *Energy, 226* (2021), 120336
[7] Xia, Y., *et al*., Numerical Investigation of Microchannel Heat Sinks with Different Inlets and Outlets Based on Topology Optimization, *Applied Energy, 330* (2023), 120335
[8] Xie, J., *et al*., A Novel Strategy to Optimize the Liquid Cooling Plates for Battery Thermal Management by Precisely Tailoring the Internal Structure of the Flow Channels, *International Journal of Thermal Sciences, 184* (2023), 107877
[9] Ravindra, J., *et al*., Hybrid Cooling of Cylindrical Battery with Liquid Channels in Phase Change Material, *International Journal of Energy Research 45* (2021), 7, pp. 11065-11083
[10] Wang, H., *et al*., Cooling Capacity of a Novel Modular Liquid-Cooled Battery Thermal Management System for Cylindrical Lithium-Ion Batteries, *Applied Thermal Engineering, 178* (2020), 115591
[11] Guo, R., *et al*., Heat Dissipation Analysis and Optimization of Lithium-Ion Batteries with a Novel Parallel-Spiral Serpentine Channel Liquid Cooling Plate, *Int. J. of Heat and Mass Transfer, 189* (2022), 122706
[12] Zhang, F., *et al*., A Novel Hybrid Battery Thermal Management System with Fins Added on and Between Liquid Cooling Channels in Composite Phase Change Materials, *Applied Thermal Engineering, 207* (2022), 118198
[13] Fang, H., *et al*., Effect of Locally Enhanced Heat Dissipation of the Polar on Li-Ion Power Batteries, *Thermal Science, 25* (2021), 4A, pp. 2713-2729
[14] Ding, Y., *et al*., Parameters of Liquid Cooling Thermal Management System Effect on the Li-Ion Battery Temperature Distribution, *Thermal Science, 26* (2022), 1B, pp. 567-577
[15] Behi, H., *et al*., Thermal Management Analysis Using Heat Pipe in the High Current Discharging of Lithium-Ion Battery in Electric Vehicles, *Journal of Energy Storage, 32* (2020), 101893
[16] Afzal, A., *et al*., Battery Thermal Management: An Optimization Study of Parallelized Conjugate Numerical Analysis Using Cuckoo Search and Artificial Bee Colony Algorithm, *International Journal of Heat and Mass Transfer, 166* (2021), 120798
[17] Feng, X., *et al*., Analysis and Optimization Control of Finned Heat Dissipation Performance for Automobile Power Lithium Battery Pack, *Thermal Science, 24* (2020), 5B, pp. 3405-3412
[18] Bernardi, D., *et al*., General Energy-Balance for Battery Systems, *Journal of The Electrochemical Society, 132* (1985), 1, pp. 5-12
[19] Narayanasamy, M. P., *et al*., Heat Transfer Analysis of Looped Micro Heat Pipes with Graphene Oxide Nanofluid for Li-Ion Battery, *Thermal Science, 25* (2021), 1A, pp. 395-405

Paper submitted: May 20, 2023
Paper revised: June 23, 2023
Paper accepted: July 9, 2023